Nighttime OClO in the winter Arctic vortex

T. Canty,[1] E. D. Rivière,[2] R. J. Salawitch,[1] G. Berthet,[2,3] J.-B. Renard,[2]
K. Pfeilsticker,[4] M. Dorf,[4] A. Butz,[4] H. Bösch,[1] R. M. Stimpfle,[5]
D. M. Wilmouth,[5] E. C. Richard,[6] D. W. Fahey,[6] P. J. Popp,[6]
M. R. Schoeberl,[7] L. R. Lait,[7] and T. P. Bui[8]

Received 18 May 2004; revised 25 August 2004; accepted 27 September 2004; published 4 January 2005.

[1] We show that a nighttime profile of OClO in the Arctic vortex during the winter of 2000 is overestimated, by nearly a factor of 2, using an isentropic trajectory model constrained by observed profiles of ClO_x (ClO + 2 × ClOOCl) and BrO. Calculated abundances of nighttime OClO are shown to be sensitive to the abundance of BrO_x (BrO + BrCl), details of the air parcel history during the most recent sunrise/sunset transitions, and the BrCl yield from the reaction BrO + ClO. Many uncertainties are considered, and the discrepancy between measured and modeled nighttime OClO appears to be robust. This discrepancy suggests that production of OClO occurs more slowly than implied by standard photochemistry. If the yield of BrCl from the reaction of BrO + ClO is increased from 7% (JPL 2002 value) to 11% (near the upper limit of the uncertainty), good agreement is found between measured and modeled nighttime OClO. This study highlights the importance of accurate knowledge of BrO + ClO reaction kinetics as well as air parcel trajectories for proper interpretation of nighttime OClO. These factors have a considerably smaller impact on the interpretation of OClO observations obtained during twilight ($90° \leq SZA \leq 92°$), when photolytic processes are still active.

Citation: Canty, T., et al. (2005), Nighttime OClO in the winter Arctic vortex, *J. Geophys. Res.*, *110*, D01301, doi:10.1029/2004JD005035.

1. Introduction

[2] Observations of OClO are used as a measure of chemical loss of polar ozone due to BrO and ClO [e.g., *Solomon et al.*, 1987; *Salawitch et al.*, 1987; *Solomon et al.*, 1989; *Wagner et al.*, 2001, 2002]. As these data are often obtained during twilight, inferences of chlorine activation and bromine levels require accurate knowledge of the twilight chemistry of OClO [*Wahner and Schiller*, 1992; *Sessler et al.*, 1995]. The SAGE III instrument, launched in December 2001, will obtain lunar occultation measurements of nighttime OClO in the polar stratosphere [*SAGE III*, 2002]. A thorough understanding of the nighttime chemistry of OClO will be needed for proper interpretation of these observations.

[3] In the winter polar stratosphere, OClO is predominantly formed through the reaction of BrO and ClO:

$$BrO + ClO \rightarrow OClO + Br \quad 59\% \quad (1a)$$

$$\rightarrow ClOO + Br \quad 34\% \quad (1b)$$

$$\rightarrow BrCl + O_2 \quad 7\% \quad (1c)$$

Percentage yields for the three branches at 195 K using JPL 2002 kinetics [*Sander et al.*, 2003] are noted. Subsequent loss of OClO is nearly all due to photolysis.

[4] To reconcile the differences between a measured nighttime lunar occultation profile of OClO [*Rivière et al.*, 2003] and modeled OClO (Figure 1a), we investigate here (1) how changes in the chemical composition of the polar vortex affect OClO; (2) the kinetics that govern formation of OClO; (3) the influence of air parcel history on OClO. To more accurately represent atmospheric conditions within the polar vortex at the time of the OClO observations, our photochemical model is constrained by measured profiles of ClO_x (ClO + 2 × ClOOCl), O_3, and temperature, as well as a profile of BrO_x (BrO + BrCl) calculated from measured BrO. All

[1]Jet Propulsion Laboratory, California Institute of Technology, Pasadena, California, USA.
[2]Laboratoire de Physique et Chimie de l'Environnement/CNRS, Université d'Orléans, Orleans, France.
[3]Now at Service d'Aéronomie du CNRS, Institut Pierre-Simon Laplace, Paris, France.
[4]Institut für Umweltphysik, University of Heidelberg, Heidelberg, Germany.
[5]Department of Chemistry and Chemical Biology, Harvard University, Cambridge, Massachusetts, USA.
[6]Aeronomy Laboratory, NOAA, Boulder, Colorado, USA.
[7]NASA Goddard Space Flight Center, Greenbelt, Maryland, USA.
[8]NASA Ames Research Center, Moffett Field, California, USA.

0148-0227/05/2004JD005035$09.00

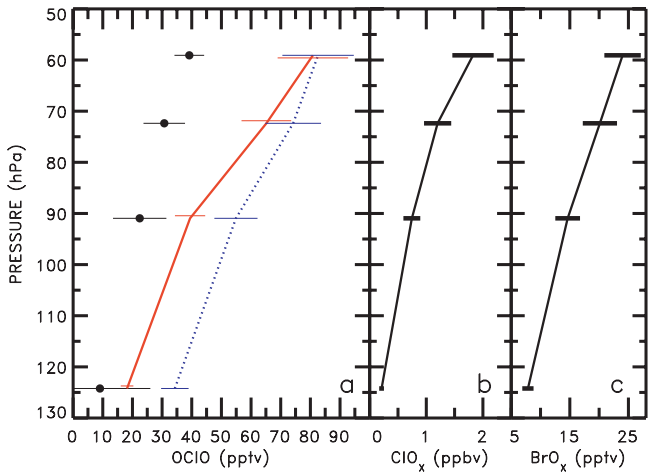

Figure 1. (a) Calculations of OClO for 1800 LT using JPL 2002 kinetics for a photochemical steady state model (blue dotted curve) and an isentropic trajectory model (red solid curve). Measured OClO (black dots) above Kiruna (68°N) at 1800 LT on January 23, 2000, using lunar occultation, is also shown. (b) ClO_x measurement from the ER-2 aircraft above Kiruna on January 20 and 27, 2000. (c) BrO_x based on DOAS measurements of BrO above Kiruna obtained on February 18, 2000. Error bars for ClO_x and BrO_x represent 1σ uncertainty; see text for description of other error bars.

observations were obtained near Kiruna, Sweden (68°N, 20°E) during the winter of 2000.

2. Model Description

[5] We use a model representation of polar ozone photochemistry designed specifically for examining the interactions between active chlorine and bromine for perturbed conditions in the polar vortex [*Salawitch et al.*, 1993]. The model calculates the temporal variation of O, ClO, ClOOCl, OClO, HOCl, BrO, BrCl, and HOBr. Profiles of reactive chlorine (ClO_x), reactive bromine (BrO_x), and ozone are specified from observations and held constant. The concentration of HO_2 is also specified, as a function of solar zenith angle (SZA), using a parameterization based on observations during the 2000 winter (formula given in caption of Figure 5 of *Hanisco et al.* [2002]).

[6] For comparisons to the measured profile of OClO, concentrations of all species are calculated, using an implicit integration scheme, along 10-day isentropic back trajectories found using 6-hour NCEP winds provided by the Goddard Space Flight Center (GSFC) Trajectory Automailer [*Schoeberl et al.*, 2000]. These trajectory calculations are initialized assuming photochemical steady state for conditions at the beginning of the trajectory. Results shown here are quite insensitive to details of the initialization. Diabatic corrections to the trajectories are not important for the present analysis because model results depend only on air mass history during the 48 hours prior to observation. For the heuristic descriptions of OClO as a function of ClO_x shown here (e.g., model results shown in Figures 2 and 4), a photochemical steady state version of the model is used (15-min time grid, implicit integration, balance of 24-hour average production, and loss of each species).

[7] JPL 2002 kinetics [*Sander et al.*, 2003] are primarily used here. The 2002 evaluation of all processes relevant to this study is the same as the 2000 evaluation, but we denote these calculations as "JPL 2002" to emphasize use of the latest evaluation. Model results for JPL 1997 [*DeMore et al.*, 1997] are also shown. The main difference between these evaluations, with regard to OClO, is consideration of the *Turnipseed et al.* [1991] study of reactions (1a)–(1c) by the JPL 2000 evaluation. This consideration increases the BrCl yield of the BrO + ClO reaction from 6% to 7% (at 195 K). We also show model results where the BrCl yield from BrO + ClO is varied. For these cases, the 2002 overall rate is used and the BrCl yield is increased at the expense of the OClO yield.

[8] Chemistry of NO_x is not included in our calculations because levels of NO_x are believed to be essentially zero based on theory [e.g., *Salawitch et al.*, 1993, Figure 5c] and ER-2 observations inside the activated Arctic vortex during winter 1988–1989 [*Fahey and Kawa*, 1990], winter 1991–1992 [*Toohey et al.*, 1993], and winter 1999–2000 (see Appendix A). The nonzero values of NO_2 (~0.1 ppbv) reported by *Rivière et al.* [2003] coincident with elevated OClO are difficult to understand based on known chemistry. Observations from the ER-2, for the range of pressure considered here, indicate that the mixing ratio of $ClONO_2$ was essentially zero (e.g., less than the detection limit of 20 pptv) over Kiruna on January 23, 2000 (these measure-

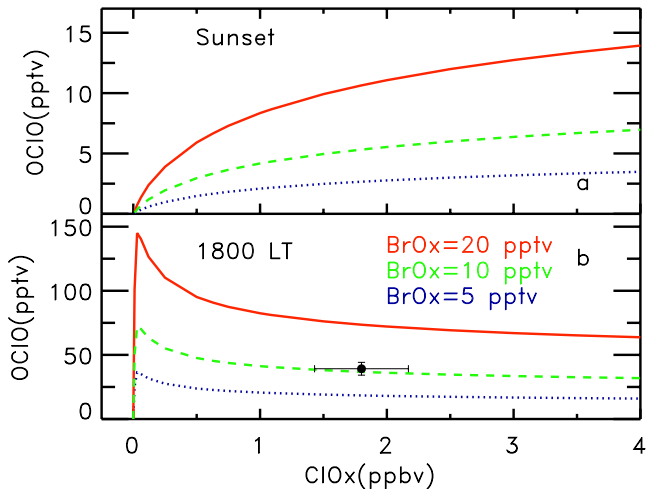

Figure 2. (a) Calculations of OClO at sunset (SZA = 90°) for a range of ClO_x and for BrO_x values of 20 pptv (red curve), 10 pptv (green dashed), and 5 pptv (blue dotted). All calculations are for pressure = 59 hPa, temperature = 195 K, solar declination = −19.4°, and latitude = 68°N assuming photochemical steady state over a 24-hour period. (b) Same as Figure 2a, but for nighttime (1800 LT, 2 hours after sunset) OClO. The data point indicates measured OClO at 59 hPa as well as measured ClO_x, from the ER-2 aircraft, at this pressure level. Model results are essentially identical to the indicated curves for all times when the atmosphere is completely dark.

Table 1. Measured Profile of OClO (*meas*) as Well as Calculated OClO Using the 10-Day Isentropic Back Trajectory Model (*traj*) and a Photochemical Steady State Box Model (*ss*)[a]

Pressure, hPa	$OClO_{meas}$, pptv	$OClO_{traj}$, pptv	$OClO_{ss}$, pptv
124.23	9.0(17)	18.18(2.1)	34.3(4.6)
90.95	22.5(9)	39.44(5.1)	54.9(7.3)
72.37	31.0(7)	65.16(8.4)	74.2(9.4)
59.08	39.2(5)	80.85(11.9)	82.6(12.0)

[a]The observation of OClO was obtained on January 23, 2000 (solar declination equal to −19.39°) at 68°N, 20°E, at 1800 LT (local time). Measurement uncertainties (1σ) are in parentheses for $OClO_{meas}$. Model uncertainty (1σ) given in parentheses for $OClO_{traj}$ and $OClO_{ss}$ reflects uncertainties due to measured ClO_x and BrO_x only.

ments were obtained by the instrument described in *Stimpfle et al.* [1999]). Furthermore, profiles of NO measured over Kiruna on January 20 and 27, 2000 (illustrated in Appendix A), are indistinguishable from zero, which supports our modeling approach. Measurements of NO are not available for the ER-2 flight on January 23, 2000.

3. Measurements

[9] Table 1 gives the profile of OClO measured over Kiruna on January 23, 2000 at 1800 Local Time (LT) (2 hours after sunset) using lunar occultation [*Rivière et al.*, 2003]. These observations were obtained using the SALOMON instrument over Kiruna on January 23, 2000, between ∼50 and ∼150 hPa. Details of the SALOMON instrument (SALOMON is an acronym for Spectroscopie d'Absorption Lunaire pour l'Observation des Minoritaires Ozone et NO_x), a balloon-borne UV-visible spectrometer, are provided by *Renard et al.* [2000]. The uncertainties (1σ) have been computed by considering both systematic instrument errors and residuals to the spectral fit [*Rivière et al.*, 2003].

[10] The model calculations are constrained by the profiles of BrO_x and ClO_x given in Table 2. The ClO_x profile is based on resonance fluorescence observations of ClO and ClOOCl from an instrument aboard the NASA ER-2 aircraft [*Stimpfle et al.*, 2004]. An average of 4 profiles of ClO_x obtained on ascent and descent above Kiruna, Sweden on January 20 and 27, 2000 is used. The statistical standard deviation of these profiles is quite small (much less than 20%) and is not considered in our error analysis. The estimated total measurement uncertainty of ClO_x is ±20% (1σ), represented in Table 2, which is considered in the uncertainty analysis for nighttime OClO. This estimate is based on factors such as the efficiencies of the conversion of ClO to Cl and of ClOOCl to Cl (the species actually detected), possible secondary reactions, and Rayleigh scattering [*Stimpfle et al.*, 2004]. The ER-2 also flew on January 23, 2000, the day of the OClO observations. However, measurements of ClOOCl were not obtained on this flight.

Table 3. Conditions for the DOAS Measurement of BrO on February 18, 2000, at Latitude Equal to 68°N and Solar Declination Equal to −11.55°[a]

Temp., K	Press., hPa	O_3, ppmv	SZA	BrO, pptv
207	124.23	1.38	83.22	7.0(0.79)
205	90.95	1.65	83.69	11.7(1.38)
204	72.37	2.24	84.02	15.3(1.67)
202	59.08	2.80	84.33	17.8(2.14)

[a]Measurement uncertainty (1σ) is in parentheses.

Scientific results presented here would be very similar had we used a profile of ClO_x inferred from measured ClO on January 23, or had we used an individual profile of ClO_x. Profiles of temperature and pressure [*Scott et al.*, 1990] as well as O_3 [*Richard et al.*, 2001] were also measured by instruments aboard the ER-2 and are used as model constraints (see Table 2). The uncertainty and standard deviation of each of these measurements is tiny and has no bearing on the conclusions of this study.

[11] The BrO_x profile given in Table 2 is calculated using the DOAS (Differential Optical Absorption Spectroscopy) balloon-borne measurement of BrO (Table 3), obtained over Kiruna on February 18, 2000. Profiles of BrO were determined from radiances between 346 and 360 nm using a grating spectrometer with a resolution of ∼0.5 nm. For the calculation of BrO_x, we used a profile for O_3 measured on February 18, 2000 by DOAS (Table 3) and a profile for ClO_x from the ER-2 over Kiruna that was measured ∼20 days earlier (Table 2). The calculation of BrO_x is relatively insensitive to ClO_x, provided that the vortex is activated and NO_x levels are low. Therefore the changes in ClO_x that may have taken place between these ER-2 flights and the DOAS flight have no significant effect on the calculation of BrO_x or our overall conclusions.

[12] The uncertainty for the profile of BrO_x given in Table 2 reflects an RSS (root sum square) propagation of the uncertainties in measured ClO_x and BrO (this overall uncertainty is dominated by the uncertainty in BrO). The estimated uncertainty of BrO (1σ) given in Table 3 is based on factors such as residuals to the spectral fits [*Fitzenberger*, 2000]. A detailed discussion of the uncertainties in measuring BrO using the DOAS technique is given by *Ferlemann et al.* [2000]. We use this profile of BrO_x for analysis of the January 23 observations of OClO because both measurements were obtained deep in the vortex and there was little descent of air over this time period, based on long-lived tracer observations from the ER-2 [*Ray et al.*, 2002].

4. Measured and Modeled OClO

[13] Figure 1a shows a comparison of the measured profile of nighttime OClO (1800 LT) to two model calculations both of which use JPL 2002 kinetics: a photo-

Table 2. Model Inputs for the January 23, 2000, Simulation of OClO[a]

Temperature, K	Pressure, hPa	Latitude, °N	Longitude, °E	O_3, ppmv	ClO_x, ppbv	BrO_x, pptv
204.0	124.23	68.9	29.5	0.91	0.21(0.04)	7.85(0.89)
200.5	90.95	68.7	29.3	1.75	0.75(0.15)	14.63(1.77)
197.0	72.37	68.5	28.9	2.08	1.2(0.24)	20.13(2.3)
194.5	59.08	68.4	28.7	2.71	1.8(0.37)	24.0(3.1)

[a]Uncertainty estimates (1σ) for the measurement of ClO_x and calculated profiles of BrO_x are in parentheses.

chemical steady state simulation, and an isentropic trajectory model simulation. Profiles of BrO_x and ClO_x used in each simulation are also shown (numerical values given in Table 2). The uncertainty estimates for calculated OClO shown in Figure 1 represent an RSS propagation of the uncertainties in BrO_x and ClO_x. Numerical values of these model result are given in Table 1.

[14] Both model simulations overestimate the measured abundance of nighttime OClO by an amount larger than can be accounted for by measurement uncertainty in the profiles of BrO_x and ClO_x used to constrain the calculations. The validity of the BrO_x profile inferred from measured BrO is discussed below (nighttime OClO is much more sensitive to variations in BrO_x than to variations in ClO_x). Also, we compare our present model results to prior simulations of the same nighttime OClO profile, which lacked constraints from observations of BrO. Nighttime OClO is sensitive to a number of other factors, in addition to BrO_x and ClO_x, such as the branching ratios of the BrO + ClO reaction and subtle details of the air parcel history prior to observation. We explore the factors that regulate nighttime OClO in the sections to follow.

[15] Isentropic trajectory model simulations are required to obtain meaningful comparisons with measurements of nighttime OClO that are obtained near the polar terminator (e.g., the region of air for which noontime solar zenith angle is between 92 and 95°), as discussed in section 4.3. Nonetheless, some of the calculations presented below make use of the photochemical steady state (PSS) model which can quickly generate the large number of model runs needed for the heuristic figures (described in the following section). The results presented below are meant to be illustrative of the general behavior of OClO (which is captured well by the PSS approach).

4.1. Influence of BrO_x and ClO_x

[16] Figure 2a shows the calculated dependence of OClO at sunset (SZA = 90°) on abundances of BrO_x and ClO_x. These calculations were conducted using the photochemical steady state model for conditions of the OClO observations at 59 hPa (further details given in the caption). Once ClO_x exceeds a certain threshold (~2 ppbv, depending on BrO_x), calculated OClO depends primarily on BrO_x. Prior to reaching this threshold, OClO at sunset grows with increasing ClO_x. Calculated OClO at sunrise behaves in a manner very similar to OClO at sunset. This view of sunrise/sunset OClO photochemistry is consistent with results presented in many previous studies [e.g., *Wahner and Schiller*, 1992; *Sessler et al.*, 1995].

[17] Figure 2b shows the dependence of calculated nighttime OClO on BrO_x and ClO_x. The behavior of nighttime OClO with increasing ClO_x is quite different than the variations exhibited by sunrise/sunset OClO. This behavior poses a complication for the quantitative use of nighttime OClO observations [e.g., *Sessler et al.*, 1995]. For values of ClO_x greater than ~0.1 ppbv, increasing ClO_x leads to a decrease in calculated nighttime OClO. This behavior is due to the detailed timing of the sequestration of BrO into BrCl versus the early evening buildup of OClO. The photolysis of BrCl shuts down earlier (SZA ≈ 92°) than the photolysis of OClO (SZA ≈ 94°). The key factor in determining nighttime OClO is the amount of BrO that is present during late twilight (92° ≤ SZA ≤ 94°). Increases in ClO_x increase the rate at which BrO is converted to BrCl during early twilight (90° to 92°). Consequently, calculated nighttime OClO decreases as ClO_x rises because less BrO is available to form OClO [e.g., *Sessler et al.*, 1995].

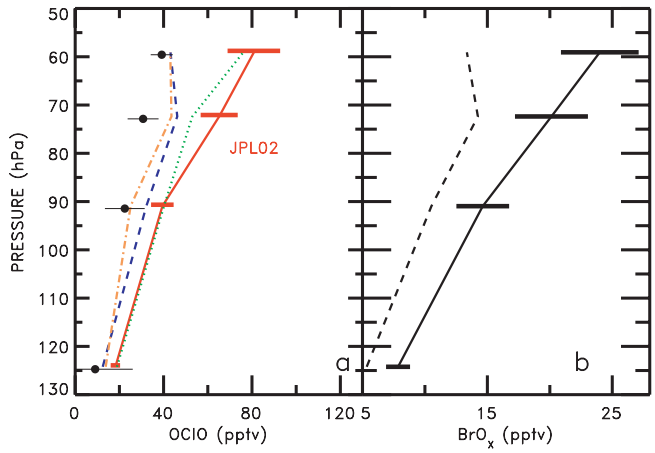

Figure 3. (a) Calculations of OClO for 1800 LT from an isentropic trajectory model using JPL 2002 kinetics and DOAS BrO_x and GSFC trajectories (red curve); DOAS BrO_x and ECMWF trajectories (green dotted curve); REPROBUS BrO_x and GSFC trajectories (blue dashed curve); REPROBUS BrO_x and ECMWF trajectories (orange dashed dotted curve). Measured OClO (black dots) above Kiruna (68°N) at 1800 LT on January 23, 2000, using lunar occultation, is also shown. (b) DOAS BrO_x (e.g., BrO_x inferred from the DOAS BrO profile) (black solid curve) and REPROBUS BrO_x (BrO_x from a 3-D model, based on decomposition of organic bromine compounds) (black dashed curve).

[18] The measured abundance of nighttime OClO at 59 hPa and the associated abundance of ClO_x are indicated by the data point on Figure 2b. Taken at face value, this data point suggests the level of BrO_x was approximately 10 pptv. Similar results are found using the isentropic trajectory model (e.g., the two model curves in Figure 1 converge to about the same point for calculated OClO at 59 hPa). The DOAS observations of BrO indicate the presence of 17.8 ± 2.14 pptv at this pressure level, from which we infer BrO_x = 24.0 ± 3.1 pptv. Clearly, there is an inconsistency between the measurements of nighttime OClO, early morning BrO, ClO_x, and the model results shown in Figure 2b. This discrepancy motivates the rest of our analysis.

[19] We connect our study here to that of *Rivière et al.* [2003], who reported reasonably good agreement between measured and modeled OClO using JPL 1997 kinetics. Figure 3a compares the measured profile of nighttime OClO to four model calculations, all using our isentropic trajectory model: one calculation is constrained by the profile for BrO_x inferred from measured BrO and air mass history from the GSFC Automailer, the second is constrained by the calculated profile of BrO_x used by *Rivière et al.* [2003] and GSFC air mass histories; the third uses BrO_x from measured BrO and air mass histories from European Centre for Medium-Range Weather Forecasts (ECMWF) winds (e.g.,

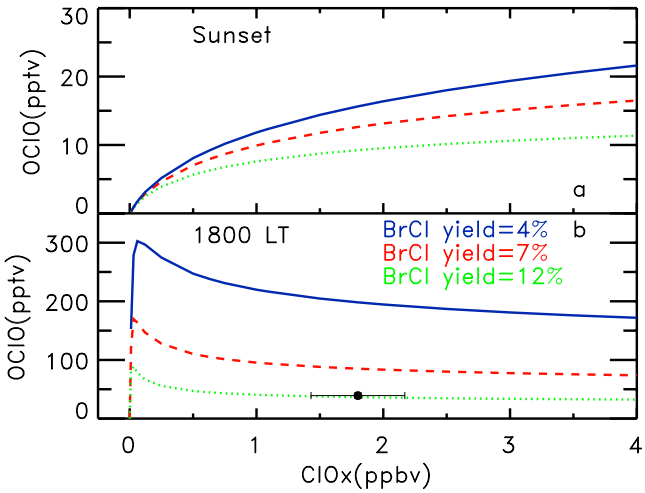

Figure 4. (a) Calculations of OClO at sunset for a range of ClO_x and for BrCl yields of 4% (blue curve), 7% (red dashed), and 12% (green dotted) from the reaction of BrO + ClO. Model constraints are the same as in Figure 2, with BrO_x = 24 pptv. (b) Same as Figure 4a, but for nighttime (1800 LT) OClO. The data point indicates measured OClO at 59 hPa as well as measured ClO_x, from the ER-2 aircraft, at this pressure level.

the same trajectories used in the Rivière et al. study); the fourth profile is constrained by the BrO_x used by *Rivière et al.* [2003] and ECMWF winds. The two profiles of BrO_x are shown in Figure 3b. Most of the differences between the calculations presented here, and those in *Rivière et al.* [2003], are due to differences in the profile of BrO_x. The different sources for air mass history have a negligible effect on model results, except for 72.37 hPa, where calculated OClO is lower using ECMWF winds. The model profile using the same constraints as in *Rivière et al.* [2003] show good agreement with their study. The calculations shown here use JPL 2002; the slightly lower BrCl yield from BrO + ClO recommended by JPL 1997 would shift the OClO model calculations higher by about 30%.

[20] The BrO_x profile used by *Rivière et al.* [2003] was based on initial values for Br_y taken from the REPROBUS chemical transport model [*Lefèvre et al.*, 1998]. The peak levels of this BrO_x profile correspond to abundances of total stratospheric Br_y that would be expected based on decomposition of methyl bromide and halons [*World Meteorological Organization* (*WMO*), 2003, Figure 1–8]. Estimates of total stratospheric Br_y based on direct observations of BrO have historically exceeded estimates based on the decomposition of methyl bromide and halons by approximately 4 to 7 pptv [*WMO*, 2003, Figure 1–8; *Pfeilsticker et al.*, 2000, Figure 2; *Wamsley et al.*, 1998, Figure 7]. This offset may represent the influence on stratospheric Br_y of species such as CH_2Br_2 and CH_2BrCl [e.g., *Wamsley et al.*, 1998], $CHBr_3$ [e.g., *Dvortsov et al.*, 1999], or the direct transport of BrO across the tropopause [e.g., *Ko et al.*, 1997; *Pfeilsticker et al.*, 2000]. The ~10 pptv offset at 59 hPa between BrO_x inferred from DOAS BrO and BrO_x from the REPROBUS model could reflect such influences on stratospheric Br_y as well as differences in the degree of descent between the atmosphere and the REPROBUS model for January 2000.

[21] The peak level of BrO_x inferred from the DOAS measurement of BrO is on the upper end of the range of accepted abundances for contemporary stratospheric Br_y [*WMO*, 2003]. For these polar conditions, we expect negligible abundances of HOBr, HBr, $BrONO_2$, and Br compared to the overall budget of Br_y. Therefore the empirically derived profile of BrO_x appears to be reasonable. The profile of BrO_x used by *Rivière et al.* [2003] is on the lower end of accepted abundances for contemporary stratospheric Br_y [*WMO*, 2003] and is therefore also reasonable. The differences in calculated nighttime OClO shown in Figure 3a provide a nice illustration of the potential role of nighttime OClO to constrain stratospheric levels of BrO_x. For the rest of our analysis, we will proceed using the empirically derived profile of BrO_x, along with its estimated uncertainty. Our results that follow are contingent on the accuracy of the DOAS measurement of stratospheric BrO.

4.2. BrCl Yield

[22] We focus here on the sensitivity of calculated OClO to the percentage yields of the three branches of BrO + ClO (reactions (1a)–(1c)). There is considerable uncertainty in the BrCl yield of this reaction. This affects the interpretation of both sunrise/sunset and nighttime OClO, but is often not considered in analysis of these measurements. In fact, the only published study that we are aware of that explores this sensitivity is *Salawitch et al.* [1987], which focused on an analysis of column OClO measured from McMurdo Station, Antarctica.

[23] The dependence of OClO on the branching ratios of reactions (1a)–(1c) occurs because channel (1a) is the primary route for formation of OClO. Most importantly, channel (1c), the BrCl branch, provides a route for the sequestration of BrO into its primary nighttime reservoir during perturbed conditions in the polar vortex. Production of OClO ceases once BrO is converted to BrCl. Model results presented below are expressed as a function of BrCl yield because (1) the kinetics changes explored here result in large variations in BrCl production (minor channel) and small variations in OClO production (major channel); (2) BrCl production regulates twilight BrO, and hence nighttime levels of OClO.

[24] Variations in the BrCl yield have only a modest effect on OClO at sunset and sunrise. Figure 4a shows steady state calculations of OClO at sunset and at 1800 LT, as a function of ClO_x, for three kinetic cases. The 7% BrCl yield is representative of standard JPL 2002 kinetics. Also shown are calculations for yields of 4% and 12%, lower and upper limits of the yield from JPL 2002 for 195 K. The temperature variations of the BrCl yield from reactions (1a)–(1c) for JPL 2002 and JPL 1997 kinetics, together with uncertainty estimates, is shown in Figure 5. A description of how the uncertainty estimates were calculated is given in Appendix B. For a range of ClO_x at sunset (Figure 4a), changes to the BrCl branching ratio lead to modest changes in OClO with a 50% decrease of the branching ratio increasing OClO by about 6 pptv.

[25] Variations in the BrCl yield from reactions (1a)–(1c) have a considerable effect on nighttime OClO. Calculated

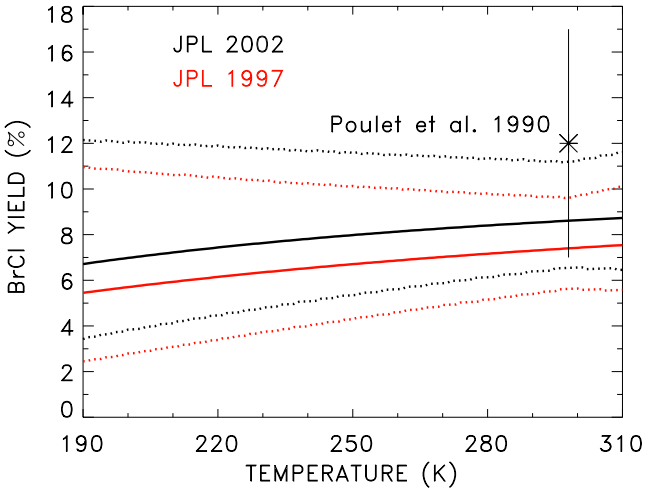

Figure 5. BrCl yield from the BrO + ClO reaction (black solid) and uncertainties (black dotted; see Appendix B) calculated using JPL 2002 kinetics and using JPL 1997 kinetics (red curves). A direct measurement of the BrCl yield reported by *Poulet et al.* [1990] at 298 K is also shown.

OClO increases by almost 200 pptv as this yield is varied from its lower limit (4%) to its upper limit (12%) (Figure 4b). The data point in Figure 4b represents observed values of nighttime OClO and ClO_x at 59 hPa. Assuming the validity of our estimate for BrO_x of 24 pptv, this data point is consistent with a BrCl yield of 12% from reactions (1a)–(1c) (using the PSS approach). In the section to follow, we show that overall consistency between measured OClO and calculations using the isentropic trajectory model is achieved for a BrCl yield of 11%. Further comments on whether the BrCl yield from this reaction truly might be as large as 11% and the implications of this yield for polar ozone loss are given in section 5 (Discussion).

4.3. Air Parcel History

[26] Figure 1, discussed earlier, showed that calculated OClO was lower using the isentropic trajectory model, compared to a photochemical steady state approach. Here we illustrate the cause of these differences and describe the sensitivity of nighttime OClO to air parcel history.

[27] The cause of the differences in calculated OClO between the trajectory and photochemical steady state approaches is primarily due to SZA history, as illustrated in Figure 6. The top panel indicates SZA history for the 12 hours prior to observation. The photochemical steady state (PSS) model reaches a minimum SZA (SZA_{min}) of 87.8° (blue solid curve), because the air mass is assumed to be stationary at 68.4°N. However, the isentropic back trajectory indicates SZA_{min} of 92.67°, due to zonal asymmetries in the computed flow (red dotted line). To assess uncertainties in the isentropic back trajectory model estimates of air parcel history, we have initialized the model with a cluster of points distributed in a ±1° latitude, ±1° longitude circle surrounding the measurement location. The gray shaded region of the top panel indicates the range of SZA histories for this cluster of trajectories.

[28] Since the air mass considered by the isentropic trajectory model did not experience $SZA_{min} < 90°$ for the day prior to observation, the amount of OClO that had built up in previous days was only partially removed by photolysis. Conversely, the PSS simulation experienced enough sunlight to completely remove the amount of OClO that had built up from the previous day. Most importantly, the level of calculated BrO in the trajectory simulations is much lower than found in the PSS case, due to differences in the photolysis of BrCl during twilight. The SZAs for the PSS simulation result in nearly complete photolysis of BrCl, leading to high levels of BrO that result in reformation of nighttime OClO after sunset (Figure 6). In contrast, the lower abundances of BrO carried into the final twilight stage within the trajectory model simulations result in smaller amounts of nighttime OClO. Calculated abundances of ClO and ClOOCl for these model runs are also shown in Figure 6.

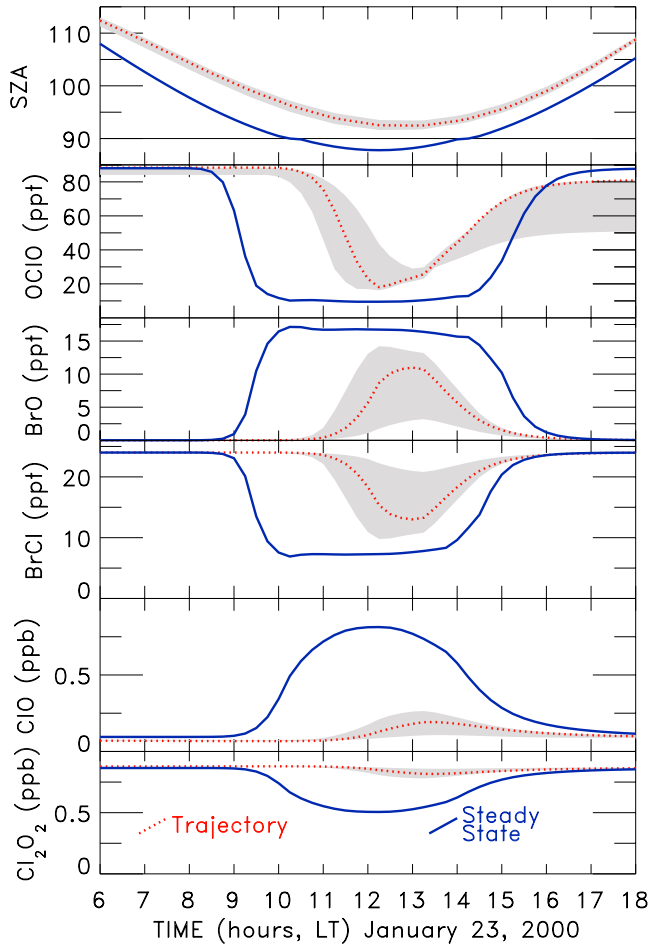

Figure 6. (top) Solar zenith angles used in the trajectory model (red dotted curve) and the steady state model (blue curve) for the 12 hours prior to the time of the OClO measurements. The gray shaded region indicates the extrema of SZA history based on an analysis of a cluster of trajectories initialized in a circle, centered on the measurement location, with a radius of ±1° latitude and ±1° longitude. (second from top) Calculated OClO using the trajectory model, the steady state model, and the trajectory cluster. Other panels show calculated values of BrO, BrCl, ClO, and ClOOCl (as indicated).

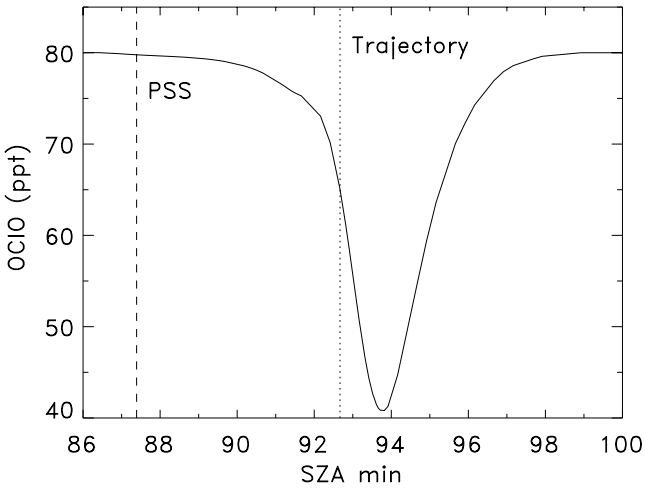

Figure 7. Value of OClO calculated at the time of measurement (1800 LT) as a function of minimum solar zenith angle (SZA) during the last 12 hours of the 10-day, isentropic trajectory model simulation at 59 hPa. This relation was found by perturbing the SZA history of an isentropic trajectory initialized at the time and place of measurement, by a series of offsets for the 12-hour period. The model was then run for each of these perturbed SZA histories. The dotted line indicates the SZA_{min} for the "base case" isentropic trajectory model. The dashed line shows SZA_{min} for the photochemical steady state simulation.

[29] The differences between the trajectory and PSS calculations, as well as the considerable spread in nighttime OClO found for the trajectory cluster simulations, are ultimately driven by differences in the wavelength dependence of BrCl and OClO photolysis. When air masses are exposed to SZA_{min} between 92° and 95°, OClO is photolyzed more efficiently than BrCl. It is possible to envision a case where an air parcel exposed to solar conditions entirely in this SZA_{min} range could lose a substantial fraction of its nighttime OClO due to photolysis, without replenishment from BrO reacting with ClO.

[30] This scenario is explored in Figure 7, which illustrates the calculated abundance of OClO for conditions of the nighttime observations at 59 hPa, as a function of SZA_{min}. This relation was calculated by perturbing the SZA versus time of the isentropic trajectory (base case) by small offsets only for the last 12 hours of the 10-day period. The SZA_{min} of the trajectory (base case) and of the PSS simulation are indicated in Figure 7. This relation indicates (1) some caution must be exercised in our interpretation of the *Rivière et al.* [2003] observations of OClO, because errors in the trajectory model (difficult to truly evaluate) can lead to large sensitivity in calculated OClO; (2) proper interpretation of nighttime OClO measurements, such as those that will be obtained by SAGE III, requires air parcel trajectory analysis, particularly if the observations are obtained near the polar terminator (the annulus of air for which SZA_{min} during a 24-hour period is between 92 and 95°).

[31] We have repeated the calculations allowing for the presence of tropospheric clouds in the J value calculation, which obscures sunlight during twilight and could conceivably lead to further complications. The model results for OClO are similar to the clear sky case shown in Figure 7. Consequently, uncertainty involving the presence of tropospheric clouds should not affect the interpretation of nighttime OClO.

[32] Errors in air mass history based on meteorological wind fields are difficult to quantify. Typically, initialization of a cluster of back trajectories surrounding a measurement location is one approach for examining the sensitivity of model results to air parcel history [e.g., *Drdla and Schoeberl*, 2003]. The discrepancy between model and measured OClO is significantly reduced for the few trajectories that possess a SZA history that leads to photolysis of OClO during twilight, but little replenishment of OClO since BrCl is not photolyzed. We believe it is unlikely that the sampled air masses would have followed precisely this SZA history at each of the four pressure levels. The thin red error bars in Figure 8a (discussed in detail in the following section) were calculated using a cluster of back trajectories and denote the range of OClO we could expect based on uncertainties in air mass history. The significance of the discrepancy between modeled and measured OClO is bolstered by the finding that model results using ECMWF winds, initialized at the precise measurement locations, produce similar results as found using GSFC winds.

4.4. Synthesis

[33] Figure 8 compares the measured nighttime OClO profile to three calculations using the isentropic trajectory model. Here, we synthesize the results of the previous sections into a single comparison, relying on the observed profiles of BrO_x and ClO_x to constrain the model. Model

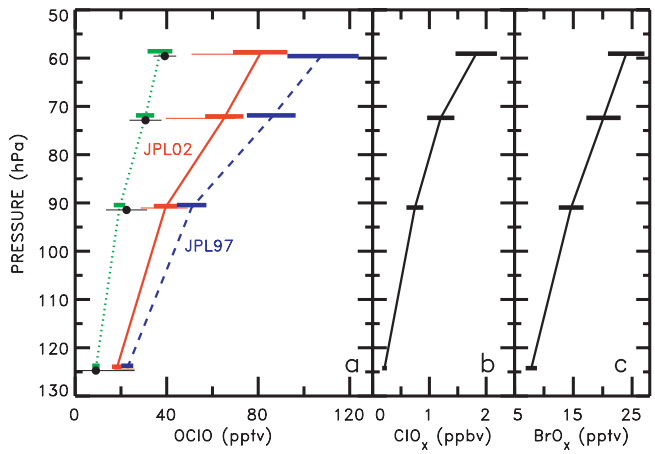

Figure 8. (a) Calculations of OClO for 1800 LT using JPL 1997 kinetics (blue dashed curve), JPL 2002 kinetics (red solid), and JPL 2002 kinetics with a BrCl yield of 11% (green dotted) at 68°N for January 23, 2000, from a 10-day isentropic back trajectory photochemical model. Measured OClO (black dots) above Kiruna (68°N) at 1800 LT on January 23, 2000, using lunar occultation, is also shown. (b) ClO_x measurement above Kiruna on January 20 and 27, 2000. (c) BrO_x based on DOAS measurements of BrO above Kiruna obtained on February 18, 2000. Error bars for ClO_x and BrO_x represent 1σ uncertainty; see text for description of other error bars.

results are shown for JPL 1997 and JPL 2002 kinetics. Both simulations overestimate the observed profile of OClO by considerable amounts. The JPL 1997 simulation results in higher abundances of OClO, because the BrCl yield from reactions (1a)–(1c) is smaller (6% at 195 K) than the yield using JPL 2002 kinetics (7% at 195 K). A model simulation using a 11% BrCl yield results in good agreement with measured nighttime OClO at all altitudes.

[34] Uncertainties in measured and modeled OClO are indicated in Figure 8. The uncertainty in measured OClO has been computed by considering systematic instrument errors and residuals to spectral fits; errors bars represent 1σ total uncertainty [*Rivière et al.*, 2003]. The thick error bars shown for each model curve represent 1σ estimates of the uncertainty in calculated OClO that are due to uncertainties in the BrO_x and ClO_x profiles used to constrain the model. As discussed in section 4.3, slight uncertainties in air parcel history can have an important effect on the interpretation of nighttime OClO. This uncertainty is represented by the thin error bars shown in Figure 8 (only for the JPL 2002 case, for clarity). This error bar reflects the range of calculated nighttime OClO for a cluster of trajectories initialized around the ±1° latitude/longitude circle surrounding the measurement location.

[35] Considering all of the error terms, the disagreement between measured and modeled OClO for JPL 2002 kinetics is barely significant at the 1σ level. Assuming the validity of the BrO_x profile and the representativeness of its error bars, measured and modeled OClO are in reasonable agreement if the minimum SZA experienced by each air parcel happened to be just equal to the value that gives lowest calculated abundance of OClO (see section 4.3). However, the tendency for the base case (trajectories initialized at the precise measurement time and location) to systematically overestimate measured OClO at each altitude, using either GSFC or ECMWF winds, leads us to believe that there is a significant discrepancy between measured and modeled nighttime OClO. More measurements of nighttime OClO, acquired at a range of SZA histories (e.g., during different phases of arctic winter if acquired from Kiruna) together with simultaneous, accurate measurements of BrO and ClO are needed to understand if this discrepancy is robust. We believe that future simultaneous observations of nighttime OClO, BrO, and ClO from suborbital platforms will greatly enhance efforts to validate the lunar occultation observations of nighttime OClO that will be provided by SAGE III.

[36] In the discussion section to follow, we explore further whether the BrCl yield from BrO + ClO might truly be as large as 11% (the value most consistent with the nighttime profile of OClO) and we discuss the implications of a higher yield of BrCl from this reaction. Also, we discuss other possible photochemical explanations for the apparent discrepancy between modeled and measured OClO. Finally, we describe other, previously published observations of BrO in twilight that could potentially pose significant complications to any analysis of nighttime OClO.

5. Discussion

[37] We have shown that a nighttime profile of OClO is simulated well using a model constrained by measured ClO_x and BrO if the BrCl yield from the BrO + ClO reaction is increased to 11%. *Sinnhuber et al.* [2002] showed that a discrepancy between observed and modeled BrO slant columns at high latitude spring during periods of high chlorine activation could also be explained by this same kinetics change.

[38] A BrCl yield of 11% from BrO + ClO is near the upper limit of the JPL 2002 uncertainty. This recommendation considered the laboratory studies of *Friedl and Sander* [1989] and *Turnipseed et al.* [1991]. The lowest temperature examined was 220 K. Hence all yields considered here are an extrapolation of laboratory data. Since the BrCl yield exhibits a small temperature dependence (Figure 5), the temperature extrapolation is likely to be valid. Also of interest is the laboratory study of *Poulet et al.* [1990], which measured yields of OClO and BrCl by direct detection of the products at room temperature. They reported a BrCl yield of 12 ± 5% (Figure 5). Considering this study, we believe it is possible that the yield of BrCl is ∼11% at temperatures near 195 K.

[39] *Toohey and Anderson* [1988] reported BrCl yields between 5 and 17% at room temperature, and suggested the production of BrCl proceeds through a BrOOCl intermediate that either decomposes into Br and ClOO or eliminates BrCl via a four-center transition state. They suggested the yield of BrCl from BrO + ClO might exhibit a pressure dependence due to quenching of the intermediate, a behavior consistent with their laboratory data. We have not considered a possible pressure dependence to the BrCl yield in our modeling work. This possibility must be better quantified in future laboratory investigations of this reaction.

[40] There are other implications of the much lower than expected observations of nighttime OClO. Models have historically been unable to fully account for the observed rate of chemical ozone depletion in the Arctic vortex during January [e.g., *Becker et al.*, 1998, 2000; *Rex et al.*, 2003]. Since reaction pathways (1b) and (1c) lead to catalytic loss of ozone, increasing the yield of BrCl at the expense of OClO production will lead to faster O_3 loss by the BrO + ClO cycle, for a model constrained by measured BrO [*Sinnhuber et al.*, 2002]. The 11% yield of BrCl that is consistent with nighttime OClO could therefore lead to a ∼10% increase in loss by BrO + ClO and a ∼5% increase in the total chemical loss of O_3. This would not fully solve the discrepancy described by *Becker et al.* and *Rex et al.* but, nonetheless, is important for our overall understanding of polar ozone. However, for a model constrained by BrO_x or Br_y, the increased yield of BrCl from BrO + ClO has a smaller effect on calculated ozone loss (indeed, in some instances this change can lead to smaller ozone loss rates) because BrO is buffered into BrCl.

[41] We discuss here other possible photochemical explanations for the observations of lower than expected levels of nighttime OClO. If the BrCl yield from BrO + ClO is held fixed at the recommended ratio, the yield of OClO would have to be reduced from ∼59% to 30% (at the expense of increased yield of ClOO) to match the observed profile. This kinetics change is outside of the JPL uncertainties [*DeMore et al.*, 1997; *Sander et al.*, 2003]. However, such a change would lead to a large increase in

calculated ozone loss, since the ClOO channel is part of a catalytic cycle.

[42] Another possibility that could explain the lower than expected values of nighttime OClO is the production of the BrOOCl adduct from BrO + ClO at low temperature, providing another means to sequester BrO during twilight. This channel has been examined theoretically [e.g., *Avallone and Toohey*, 2001, and references therein] but not in the laboratory. The BrOOCl adduct would have to be thermally and photolytically stable to play a role in nighttime OClO chemistry, and is not considered in the model calculations shown above.

[43] The self reaction of OClO, yielding ClOOCl and O_2, is another possible explanation for the low values of nighttime OClO. This reaction is exothermic by 61 kJ/mole, but has not been studied in the laboratory. Interestingly, it would have a much larger effect on nighttime OClO than on sunrise/sunset OClO due to the quadratic nature of the reaction. We estimate a rate constant $\sim 5 \times 10^{-13}$ cm^3 molec^{-1} s^{-1} is required to obtain good agreement with the measured profile of nighttime OClO. However, this reaction is unlikely to proceed at this rate based on the observation that it is possible to store up to 100 torr of OClO in a bulb without appreciable loss (S. Sander, private communication, 2003).

[44] Yet another possibility is the reaction of BrO with OClO to form BrOCl(O)O (J. Hansen, private communication, 2003). This reaction is also exothermic, by 33.5 kJ/mole [*Francisco and Clark*, 1998]. The reaction of ClO with OClO is exothermic by 45.6 kJ/mole and proceeds at a rate of $\sim 7 \times 10^{-13}$ cm^3 molec^{-1} s^{-1} at 195 K. Again, no laboratory kinetic studies of BrO + OClO have been carried out. Including BrO + OClO in our model, using the rate constant of ClO + OClO, has only a small effect on calculated OClO because levels of BrO are low during the time of OClO buildup.

[45] This leads us to an important possible complication for any analysis of nighttime OClO. Calculated abundances of nighttime OClO are sensitive to the time evolution of BrO during twilight. *Avallone and Toohey* [2001] presented measurements of BrO during the AASE I and II campaigns (Arctic winters of 1988/1989 and 1991/1992, respectively) that indicated the presence of $\sim$2 pptv of BrO during night. This is a much higher level than found in our model. They speculated that thermal decomposition of the BrOOCl adduct (described above) might be responsible. If levels of nighttime BrO are truly $\sim$2 pptv, this poses a significant challenge to any interpretation of nighttime OClO. In this case, production of OClO would continue at all SZA (even well after darkness) because ClO is provided from the thermal decomposition of ClOOCl.

[46] The quantification of nighttime BrO is difficult because it requires precise knowledge of any nonzero biases in the instrument (e.g., scattering of light). It is beyond the scope of this paper to pursue the consequences of the *Avallone and Toohey* [2001] observations in the context of our interpretation of nighttime OClO. We point out, however, that elevated abundances of nighttime BrO column were reported, independent of the work of *Avallone and Toohey* [2001], using direct lunar observations in the near UV spectral region [*Wahner et al.*, 1990]. A BrO channel was operating on the instrument that provided the observations of ClO_x used here. Once these data are calibrated, they will provide important additional constraints on our understanding of nighttime OClO. Since quantitative interpretation of nighttime OClO requires precise knowledge of nighttime levels of BrO, these data could be quite useful.

[47] Finally, we note that catalytic loss of ozone by cycles involving higher oxides of chlorine [*Sander et al.*, 1989] might be considered as an attractive resolution to the January ozone loss discrepancy [e.g., *Rex et al.*, 2003] because this ozone sink would be most efficient during periods of solar illumination, but at high SZA (when the discrepancy between measured and modeled ozone loss rates is largest). This behavior is caused by the involvement of OClO and photons in these cycles. Previously published model calculations indicate that these cycles play a negligible role in chemical loss of polar ozone due to the rapid thermal decomposition of Cl_2O_3 (the product of the reaction ClO + OClO), which is faster than photolysis of Cl_2O_3 [*Burkholder et al.*, 1993]. Our model calculations indicate that none of the scenarios described here alters this view of a negligible role for cycles involving higher oxides of chlorine. Given the *Rivière et al.* [2003] observations of low amounts of nighttime OClO, it is hard to conceive of a significant role for these ozone loss cycles because production of higher oxides of chlorine apparently involves reactions with OClO.

6. Conclusion

[48] Calculated profiles of nighttime OClO in the Arctic vortex during a time of chlorine activation are sensitive to: levels of BrO_x (BrO + BrCl); the branching ratios of the BrO + ClO reaction; and the air parcel history (e.g., temporal variation of SZA) during the most recent sunrise/sunset transitions. The measured abundance of nighttime OClO, obtained over Kiruna, Sweden, on January 23, 2000, is considerably less than a profile calculated using an isentropic trajectory model, constrained by a profile for BrO_x inferred from DOAS balloon-borne observations of BrO and a profile for ClO_x (ClO + 2 $\times$ ClOOCl) based on ER-2 aircraft observations of ClO and ClOOCl. This discrepancy appears to be robust considering various uncertainties: nonetheless, results of this analysis depend on the accuracy of the BrO_x profile and its associated uncertainty. A possible resolution to this discrepancy would be an 11% yield of BrCl from the BrO + ClO reaction (a slightly smaller yield than the upper limit of the JPL 2002 uncertainty) rather than the 7% yield based on JPL 2002 kinetics. This kinetics change would increase chemical ozone loss rates in the polar vortex, since production of BrCl from BrO + ClO is part of an ozone removal cycle. Many other possible photochemical resolutions to this discrepancy are discussed, although none appear likely.

[49] Proper interpretation of nighttime OClO requires accurate knowledge of daytime profiles of BrO_x and the final, nighttime value of BrO. Significant caveats must be attached to our analysis of nighttime OClO, related to uncertainties in daytime BrO_x and nighttime BrO. For example, our profile of BrO_x based on measured BrO exceeds some estimates of Br_y based on the decomposition of methyl bromide and halons. Model calculations using BrO_x from the REPROBUS model, which is lower than

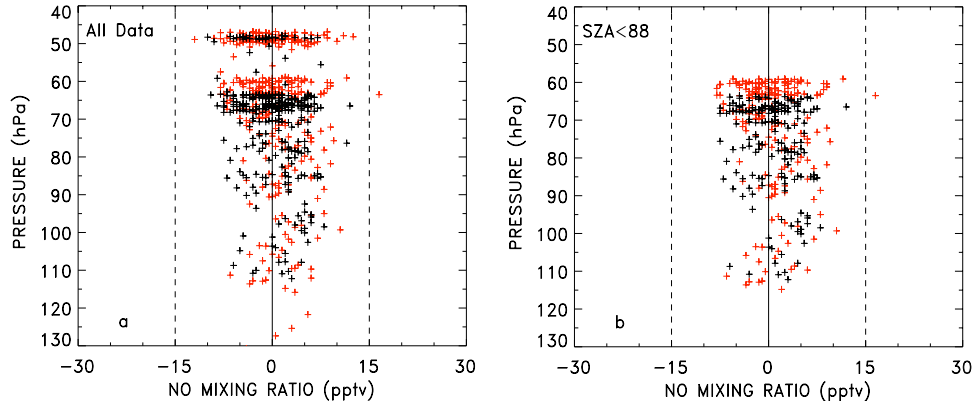

Figure A1. (a) Measurements of the mixing ratio of NO obtained on ascent and descent over Kiruna, Sweden (68°N), on January 20, 2000 (black), and January 27, 2000 (red). Measurements were obtained at 1-s intervals using a technique described by *Gao et al.* [1997]. The estimated measurement precision of the 1-s data is 15 pptv (1σ) (indicated by dashed vertical lines), and the estimated accuracy is ±6%. The data shown here have been smoothed using a 10-s median filter. (b) Same as Figure A1a, except data are shown only for conditions when solar zenith angle was less than 88°.

BrO_x based on the DOAS observations of BrO (see Figure 3b), are in good agreement with observed nighttime OClO for standard photochemistry. Constraining the model with lower values of BrO_x could alleviate the need to modify the BrCl yield. Better knowledge of stratospheric BrO will help determine how much the BrCl yield needs to be adjusted, if at all, to obtain agreement between modeled and measured nighttime OClO. Also, several previous studies have reported observations of nonzero BrO at night, which is difficult to account for with known photochemistry and which would complicate any analysis of nighttime OClO.

[50] Nighttime observations of OClO profiles in the polar vortices are planned from SAGE III lunar occultation spectra. Nighttime OClO can also be retrieved from lunar occultation spectra recorded by the Scanning Imaging Absorption Spectrometer for Atmospheric Chartography (SCIAMACHY) [*Bovensmann et al.*, 1999]. Ideally, measurements by either instrument can be used to infer profiles of BrO_x in an activated vortex. However, the branching ratios for the various pathways of the BrO + ClO reaction must be better understood before future SAGE III data can be used in this manner. Finally, future analyses of SAGE III or SCIAMACHY observations of OClO obtained near the polar terminator (the annulus of air for which SZA_{min} during a 24-hour period is between 92 and 95°) will require accurate consideration of air parcel history during the most recent sunrise/sunset transitions.

Appendix A: Profiles of NO_x Over Kiruna

[51] The high values of NO_2 (e.g., 100 to 150 pptv) measured using the SALOMON instrument over Kiruna on January 23, 2000, are difficult to reconcile with the elevated levels of OClO and known photochemical theory [*Rivière et al.*, 2003]. Elevated levels of NO_2 inside the Arctic vortex are also reported for February 2000 by a group using a different solar occultation spectrometer, the SAOZ instrument aboard a long duration balloon [*Marchand et al.*, 2003]. However, the abundance of NO_2 below 20 km was measured to be close to zero in the Arctic vortex on February 18, 2000 based on spectra from the same DOAS instrument used to measure the BrO profile used here. The DOAS profile for NO_2 on February 18, 2000 is available at http://www.iup.uni-heidelberg.de/institut/forschung/groups/atmosphere/stratosphere.

[52] The difficulty posed by nonzero levels of NO_2 inside the perturbed vortex is discussed at length by *Rivière et al.* [2003]. They present many possible chemical explanations and conclude "our results show that it is impossible to reach a simultaneous agreement between our model and measurements of NO_2 and OClO, given our present knowledge of the interaction between nitrogen and halogen species." Recently, *Rivière et al.* [2004] have pointed out that agreement between theory and observation of NO_2 and OClO could be improved if the rates of the association reactions ClO + NO_2 + M and BrO + NO_2 + M are three times slower than the standard values used in models [e.g., *Sander et al.*, 2003]. However, this change pushes both rate constants beyond JPL 2002 estimates of their respective uncertainties [*Rivière et al.*, 2004]. Furthermore, an empirical study of the relation between measured ClO, NO_2, and $ClONO_2$ for high latitude spring/summer showed good consistency with the rate constant from the JPL evaluations [*Stimpfle et al.*, 1999].

[53] The ER-2 flew from Kiruna on January 23, 2000. The in situ resonance fluorescence instrument used to measure ClO and ClOOCl is also able to quantify ambient $ClONO_2$ [*Stimpfle et al.*, 1999]. Measurements from this instrument revealed zero $ClONO_2$ (to within the 1σ detection limit of 20 pptv) on ascent and descent over Kiruna on January 23, 2000. If NO_x (NO + NO_2) had been present over Kiruna at the ∼100 pptv level, standard theory predicts rapid formation of measurable amounts of $ClONO_2$ given the high levels of ClO_x known to be present at this time.

[54] The ER-2 also carried an in situ, chemiluminescence instrument that measures NO and NO_y [*Gao et al.*, 1997; *Fahey et al.*, 2001]. This instrument did not obtain data on

January 23, 2000. However, profiles of NO measured above Kiruna on January 20 and 27, 2000, are extremely low. The inner region of the polar vortex was above Kiruna on January 20, 23, and 27 based on maps of potential vorticity and tracer measurements from the ER-2 [*Ray et al.*, 2002, Figure 4].

[55] Figure A1a shows measurements of NO obtained on ascent and descent over Kiruna on these days. The data were acquired at 1-s intervals with a measurement precision of 15 pptv. Data shown in Figure A1 have been smoothed using a 10-s median filter. The detection limit for NO is 4 pptv for a 10-s average. Much of this data was acquired after sunset, when levels of NO approach zero even in the presence of significant levels of NO_x. Therefore daytime measurements of NO are shown in Figure A1b [solar zenith angles (SZA) less than 88°]. Under these conditions, the rapid photolysis of NO_2 should lead to appreciable and measurable levels of NO if ambient NO_2 had been present at the ~100 pptv level. The observations shown in Figure A1b suggest essentially zero levels of NO_x, as expected based on standard photochemical theory for perturbed conditions in the Arctic vortex prior to nearly complete recovery of ClO back to $ClONO_2$. The apparent inconsistency between the SALOMON and SAOZ measurements of NO_2 and the ER-2 observations of NO in the Arctic vortex during late January requires further investigation.

[56] Finally, we note that the "high values of NO_2" reported by *Rivière et al.* [2003] in the Arctic vortex are equal to only ~0.1 to 0.15 ppbv of NO_x (since the observations were obtained at night). This amount of NO_x is small compared to the ~1 to 2 ppbv of ClO_x present in the vortex during late January (Figure 1b). Had we initialized our model with these levels of NO_x, we would have simply formed 0.1 to 0.15 ppbv of $ClONO_2$ within a few hours (formation of $ClONO_2$ would occur at night, due to supply of ClO from the thermal decomposition of ClOOCl). The overall levels of ClO_x would therefore be largely unperturbed. The formation of $ClONO_2$ (in the presence of 0.1 to 0.15 ppbv of NO_x) would be favored over formation of $BrONO_2$ in a perturbed vortex, given the ratio of ClO to BrO and the more rapid photolysis of $BrONO_2$ compared to $ClONO_2$. The calculated SZA dependence of BrO in our model simulations should be robust, even in the presence of fresh injection 0.1 to 0.15 ppbv of NO_x, because this NO_x would be essentially be prevented from reacting with BrO due to the rapid formation of $ClONO_2$. Consequently, our model calculations seem to be robust given our knowledge of $ClONO_2$ photochemistry.

Appendix B: Uncertainty Calculation

[57] The fractional yield of BrCl from the BrO + ClO reaction

$$BrO + ClO \rightarrow OClO + Br \quad (B1a)$$

$$\rightarrow ClOO + Br \quad (B1b)$$

$$\rightarrow BrCl + O_2 \quad (B1c)$$

is found by dividing the rate constant of reaction (B1c) by the overall rate constant for the reaction (the sum of reactions (B1a)–(B1c)).

$$BrCl_{yield} = \frac{k_{BrCl}}{k_{BrO+ClO}} = \frac{k_{1c}}{k_1} \quad (B2)$$

To determine the uncertainty in the fractional yield of BrCl, we first determine the uncertainty in the overall BrO + ClO reaction (U). This is found from the RSS combination of the absolute uncertainties (e) of the three component reactions [*Harris*, 1995].

$$U = \sqrt{(e_{1a})^2 + (e_{1b})^2 + (e_{1c})^2} \quad (B3)$$

We calculate the absolute uncertainty for each component reaction, as a function of temperature, using the JPL 2002 [*Sander et al.*, 2003] formulation.

$$e(T)_{upper} = k(T) \times f(T) \quad (B4)$$

$$e(T)_{lower} = k(T)/f(T), \quad (B5)$$

where

$$f(T) = f(298k) \exp\left[g\left(\frac{1}{T} - \frac{1}{298}\right)\right] \quad (B6)$$

For each branch of the BrO + ClO reaction, f(298 k) = 1.25 and g = 150 [*Sander et al.*, 2003]. The upper and lower bounds of the uncertainty in a rate constant are found by multiplying or dividing the rate constant by f(T).

[58] The fractional uncertainty of the overall reaction is given by

$$F_1 = \frac{U}{k_1} \quad (B7)$$

and the fractional uncertainty of the BrCl branch is given by

$$F_{1c} = \frac{e_{1c}}{k_{1c}} \quad (B8)$$

The fractional uncertainty for the BrCl yield from the reaction of BrO with ClO is then given by [*Harris*, 1995].

$$\text{BrCl yield uncertainty} = \sqrt{(F_1)^2 + (F_{1c})^2} \quad (B9)$$

The upper and lower bounds of the BrCl yield uncertainty are found using $e(T)_{upper}$ and $e(T)_{lower}$, respectively, given by equations (B4) and (B5).

[59] **Acknowledgments.** We thank K. McKinney, D. Toohey, M. Santee, M. Rex, and J. Margitan for many helpful discussions and their assistance in our use of observations from the Arctic winter of 1995 in the early part of this study. Helpful discussion with J. Hansen, R. Friedl, S. Sander, and L. Kovalenko are also greatly appreciated. This work was funded by the NASA Upper Atmosphere Research, Atmospheric Chemistry Modeling and Analysis, and Solar Occultation Satellite Science Team programs. Research at the Jet Propulsion Laboratory, California Institute

of Technology, is performed under contract with the National Aeronautics and Space Administration.

References

Avallone, L. M., and D. W. Toohey (2001), Tests of halogen photochemistry using in situ measurements of ClO and BrO, *J. Geophys. Res.*, *106*(10), 10,411–10,421.

Becker, G., R. Muller, D. S. McKenna, M. Rex, and K. S. Carslaw (1998), Ozone loss rates in the arctic stratosphere in the winter 1991/92: Model calculations compared with Match results, *Geophys. Res. Lett.*, *25*, 4325–4328.

Becker, G., R. Muller, D. S. McKenna, M. Rex, K. S. Carslaw, and H. Oelhaf (2000), Ozone loss rates in the Arctic stratosphere in the winter 1994/1995: Model simulations underestimate results of the Match analysis, *J. Geophys. Res.*, *105*, 15,175–15,184.

Bovensmann, H., J. P. Burrows, M. Buchwitz, J. Frerick, S. Noël, and V. V. Rozanov (1999), SCIAMACHY: Mission objectives and measurement modes, *J. Atmos. Sci.*, *56*, 127–150.

Burkholder, J. B., R. L. Mauldin III, R. J. Yokelson, S. Solomon, and A. R. Ravishankara (1993), Kinetic, thermochemical, and spectroscopic study of Cl_2O_3, *J. Phys. Chem.*, *97*, 7597–7605.

DeMore, W. B., et al. (1997), Chemical kinetics and photochemical data for use in stratospheric modeling, Evaluation 12, *JPL Publ.*, *97-4*.

Drdla, K., and M. R. Schoeberl (2003), Microphysical modeling of the 1999–2000 Arctic winter: 2. Chlorine activation and ozone depletion, *J. Geophys. Res.*, *108*(D5), 8319, doi:10.1029/2001JD001159.

Dvortsov, V. L., M. A. Geller, S. Solomon, S. M. Schauffler, E. L. Atlas, and D. R. Blake (1999), Rethinking reactive halogen budgets in the midlatitude lower stratosphere, *Geophys. Res. Lett.*, *26*, 1699–1702.

Fahey, D. W., and S. R. Kawa (1990), Nitric oxide measurements in the Arctic winter stratosphere, *Geophys. Res. Lett.*, *17*, 489–492.

Fahey, D. W., et al. (2001), The detection of large HNO_3-containing particles in the winter Arctic stratosphere, *Science*, *291*, 1026–1031.

Ferlemann, F., N. Bauer, R. Fitzenberger, H. Harder, H. Osterkamp, D .Perner, U. Platt, M. Schneider, P. Vradelis, and K. Pfeilsticker (2000), Differential optical absorption spectroscopy instrument for stratospheric balloonborne trace-gas studies, *Appl. Opt.*, *39*, 2377–2386.

Fitzenberger, R. (2000), Investigation of the stratospheric inorganic bromine budget for 1996–2000: Balloon borne measurements and model comparison, Differential optical absorption spectroscopy instrument for stratospheric balloonborne trace-gas studies, doctoral dissertation, Univ. of Heidelberg, Heidelberg, Germany.

Francisco, J. S., and J. Clark (1998), Study of the stability of $BrClO_3$ isomers, *J. Phys. Chem. A*, *102*, 2209–2214.

Friedl, R. R., and S. P. Sander (1989), Kinetics and product studies of the reaction ClO + BrO using discharge-flow mass spectrometry, *J. Phys. Chem.*, *93*, 4756–4764.

Gao, R.-S., et al. (1997), Partitioning of the reactive nitrogen reservoir in the lower stratosphere of the southern hemisphere: Observations and modeling, *J. Geophys. Res.*, *102*, 3935–3949.

Hanisco, T. F., J. B. Smith, R. M. Stimpfle, D. M. Wilmouth, J. G. Anderson, E. C. Richard, and T. P. Bui (2002), In situ observations of HO_2 and OH obtained on the NASA ER-2 in the high-ClO conditions of the 1999/2000 Arctic polar vortex, *J. Geophys. Res.*, *107*(D20), 8283, doi:10.1029/2001JD001024.

Harris, D. (1995), *Quantitative Chemical Analysis*, 837 pp., W. H. Freeman, New York.

Ko, M. K. W., N.-D. Sze, C. J. Scott, and D. K. Weisenstein (1997), On the relation between stratospheric chlorine/bromine loading and short-lived tropospheric source gases, *J. Geophys. Res.*, *102*, 25,507–25,517.

Lefèvre, F., F. Figarol, K. S. Carslaw, and T. Peter (1998), The 1997 Arctic ozone depletion quantified from three-dimensional model simulations, *Geophys. Res. Lett.*, *25*, 2425–2428.

Marchand, M., S. Bekki, L. Denis, J.-P. Pommereau, and B. V. Khattatov (2003), Test of the nighttime polar stratospheric NO_2 decay using wintertime SAOZ measurements and chemical data assimilation, *Geophys. Res. Lett.*, *30*(18), 1920, doi:10.1029/2003GL017582.

Pfeilsticker, K., W. T. Sturges, H. Bösch, C. Camy-Peyret, M. P. Chipperfield, A. Engel, R. Fitzenberger, M. Müller, S. Payan, and B.-M. Sinnhuber (2000), Lower stratospheric organic and inorganic bromine budget for the arctic winter 1998/00, *Geophys. Res. Lett.*, *27*, 3305–3308.

Poulet, G., T. Lancar, G. Laverdet, and G. Le Bras (1990), Kinetics and products of the BrO + ClO reaction, *J. Phys. Chem.*, *94*, 278–284.

Ray, E. A., F. L. Moore, J. W. Elkins, D. F. Hurst, P. A. Romashkin, G. S. Dutton, and D. W. Fahey (2002), Descent and mixing in the 1999–2000 northern polar vortex inferred from in situ tracer measurements, *J. Geophys. Res.*, *107*(D20), 8285, doi:10.1029/2001JD000961.

Renard, J.-B., M. Chartier, C. Robert, G. Chalumeau, G. Berthet, M. Pirre, J. P. Pommereau, and F. Goutail (2000), SALOMON: A new, light balloon-borne UV-visible spectrometer for nighttime observations of stratospheric trace-gas species, *Appl. Opt.*, *39*, 386–392.

Rex, M., R. J. Salawitch, M. L. Santee, J. W. Waters, K. Hoppel, and R. Bevilacqua (2003), On the unexplained stratospheric ozone losses during cold Arctic Januaries, *Geophys. Res. Lett.*, *30*(1), 1008, doi:10.1029/2002GL016008.

Richard, E. C., et al. (2001), Severe chemical ozone loss inside the Arctic polar vortex during winter 1999–2000 inferred from in situ airborne measurements, *Geophys. Res. Lett.*, *28*, 2197–2200.

Rivière, E. D., M. Pirre, G. Berthet, J.-B. Renard, F. G. Taupin, N. Huret, M. Chartier, B. Knudsen, and F. Lefèvre (2003), On the interaction between nitrogen and halogen species in the Arctic polar vortex during THESEO and THESEO 2000, *J. Geophys. Res.*, *108*(D5), 8311, doi:10.1029/2002JD002087.

Rivière, E. D., M. Pirre, J.-B. Renard, G. Berthet, and F. Lefèvre (2004), Investigating the halogen chemistry from high-latitude nighttime stratospheric measurements of OClO and NO_2, *J. Atmos. Chem.*, in press.

SAGE III (2002), Algorithm theoretical basis documents for solar lunar products, Version 2.1, *LaRC 475-00-109*, NASA Langley Res. Cent., Hampton, Va., 26 March. (Available from http://eospso.gsfc.nasa.gov/eos_homepage/for_scientists/atbd/docs/SAGE_III).

Salawitch, R. J., S. C. Wofsy, and M. B. McElroy (1987), Chemistry of OClO in the antarctic stratosphere: Implications for bromine, *Planet. Space Sci.*, *35*, 213–224.

Salawitch, R. J., et al. (1993), Chemical loss of ozone in the Arctic vortex of winter of 1991–92, *Science*, *261*, 1146–1149.

Sander, S. P., R. R. Friedl, and Y. L. Yung (1989), Rate of formation of the ClO dimer in the polar stratosphere: Implications for ozone loss, *Science*, *245*, 1095–1098.

Sander, S. P., et al. (2003), Chemical kinetics and photochemical data for use in atmospheric studies, Evaluation 14, *JPL Publ.*, *02-25*.

Schoeberl, M. R., L. C. Sparling, C. H. Jackman, and E. L. Fleming (2000), A Lagrangian view of stratospheric trace gas distributions, *J. Geophys. Res.*, *105*, 1537–1552.

Scott, S. G., T. P. Bui, K. R. Chan, and S. W. Bowen (1990), The meteorological measurement system on the NASA ER-2 aircraft, *J. Atmos. Oceanic Technol.*, *7*, 525–540.

Sessler, J., M. P. Chipperfield, J. A. Pyle, and R. Toumi (1995), Stratospheric OClO measurements as a poor quantitative indicator of chlorine activation, *Geophys. Res. Lett.*, *22*, 687–690.

Sinnhuber, B.-M., et al. (2002), Comparison of measurements and model calculations of stratospheric bromine monoxide, *J. Geophys. Res.*, *107*(D19), 4398, doi:10.1029/2001JD000940.

Solomon, S., G. H. Mount, R. W. Sanders, and A. L. Schmeltekopf (1987), Visible spectroscopy at McMurdo-Station, Antarctica: 2. Observations of OClO, *J. Geophys. Res.*, *92*, 8329–8338.

Solomon, S., R. W. Sanders, M. A. Carroll, and A. L. Schmeltekopf (1989), Visible and near-ultraviolet spectroscopy at McMurdo station, Antarctica: 5. Diurnal variation of BrO and OClO, *J. Geophys. Res.*, *94*, 11,393–11,403.

Stimpfle, R. M., et al. (1999), The coupling of $ClONO_2$, ClO, and NO_2 in the lower stratosphere from in situ observations using the NASA ER-2 aircraft, *J. Geophys. Res.*, *104*, 26,705–26,714.

Stimpfle, R. M., D. M. Wilmouth, R. J. Salawitch, and J. G. Anderson (2004), First measurements of ClOOCl in the stratosphere: The coupling of ClOOCl and ClO in the Arctic polar vortex, *J. Geophys. Res.*, *109*, D03301, doi:10.1029/2003JD003811.

Toohey, D. W., and J. G. Anderson (1988), Formation of BrCl ($^3Pi_0$+) in the reaction of BrO with ClO, *J. Phys. Chem.*, *92*, 1705–1708.

Toohey, D. W., L. M. Avallone, L. R. Lait, P. A. Newman, M. R. Schoeberl, D. W. Fahey, E. L. Woodbridge, and J. G. Anderson (1993), The seasonal evolution of reactive chlorine in the northern hemisphere stratosphere, *Science*, *261*, 1134–1135.

Turnipseed, A., J. W. Birks, and J. G. Calvert (1991), Kinetics and temperature dependence of the BrO + ClO reaction, *J. Phys. Chem.*, *95*, 4356–4364.

Wagner, T., C. Leue, K. Pfeilsticker, and U. Platt (2001), Monitoring of the stratospheric chlorine activation by GOME OClO measurements in the austral and boreal winters 1995 through 1999, *J. Geophys. Res.*, *106*, 4971–4986.

Wagner, T., F. Wittrock, A. Richter, M. Wenig, J. P. Burrows, and U. Platt (2002), Continuous monitoring of the high and persistent chlorine activation during the Arctic winter 1999/2000 by the GOME instrument on ERS-2, *J. Geophys. Res.*, *107*(D20), 8267, doi:10.1029/2001JD000466.

Wahner, A., J. Callies, H.-P. Dorn, U. Platt, and C. Schiller (1990), Near UV atmospheric absorption measurements of column abundances during

airborne arctic stratospheric expedition, January–February 1989: 3. BrO observations, *Geophys. Res. Lett.*, *17*, suppl., 517–520.

Wahner, W., and C. Schiller (1992), Twilight variation of vertical column abundances of OClO and BrO in the north polar region, *J. Geophys. Res.*, *97*, 8047–8055.

Wamsley, P. R., et al. (1998), Distribution of halon-1211 in the upper troposphere and lower stratosphere and the 1994 total bromine budget, *J. Geophys. Res.*, *103*, 1513–1526.

World Meteorological Organization (WMO) (2003), Scientific assessment of ozone depletion: 2002, *Rep. 47*, Global Ozone Res. and Monit. Proj., Geneva.

G. Berthet, Service d'Aéronomie du CNRS, Institut Pierre-Simon Laplace, 75230 Paris, France.

H. Bösch, T. Canty, and R. J. Salawitch, Jet Propulsion Laboratory, 4800 Oak Grove Drive, M/S 183-601, Pasadena, CA 91109, USA. (tcanty@jpl.nasa.gov)

T. P. Bui, NASA Ames Research Center, Moffett Field, CA 94035, USA.

A. Butz, M. Dorf, and K. Pfeilsticker, Institut für Umweltphysik, University of Heidelberg, D-69120 Heidelberg, Germany.

D. W. Fahey, P. J. Popp, and E. C. Richard, Aeronomy Laboratory, NOAA, Boulder, CO 80303, USA.

L. R. Lait and M. R. Schoeberl, NASA Goddard Space Flight Center, Greenbelt, MD 20771, USA.

J.-B. Renard and E. D. Rivière, Laboratoire de Physique et Chimie de l'Environnement/CNRS, Université d'Orléans, F-45071 Orleans, France.

R. M. Stimpfle and D. M. Wilmouth, Department of Chemistry and Chemical Biology, Harvard University, Cambridge, MA 02138, USA.